DTU Library

Autonomous control of metabolic state by a quorum sensing (QS)-mediated regulator for bisabolene production in engineered E. coli

Kim, Eun-Mi; Min Woo, Han; Tian, Tian; Yilmaz, Suzan; Javidpour, Pouya; Keasling, Jay; Soon Lee, Taek

Author's Accepted Manuscript

Autonomous control of metabolic state by a quorum sensing (QS)-mediated regulator for bisabolene production in engineered *E. coli*

Eun-Mi Kim, Han Min Woo, Tian Tian, Suzan Yilmaz, Pouya Javidpour, Jay D. Keasling, Taek Soon Lee
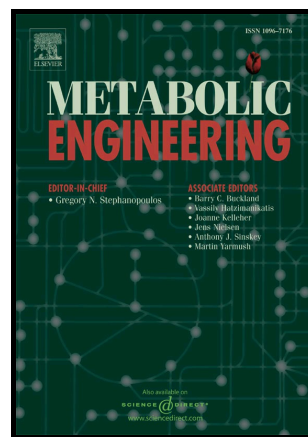
Cite this article as: Eun-Mi Kim, Han Min Woo, Tian Tian, Suzan Yilmaz, Pouya Javidpour, Jay D. Keasling and Taek Soon Lee, Autonomous control of metabolic state by a quorum sensing (QS)-mediated regulator for bisabolene production in engineered *E. coli*, *Metabolic Engineering*, https://doi.org/10.1016/j.ymben.2017.11.004

Autonomous control of metabolic state by a quorum sensing (QS)-mediated

regulator for bisabolene production in engineered *E. coli*

Eun-Mi Kim[a,b], Han Min Woo[a,b1], Tian Tian[a,b], Suzan Yilmaz[a,c], Pouya Javidpour[a,b], Jay D. Keasling[a,b,d,e,f], Taek Soon Lee[a,b*]

[1]Joint BioEnergy Institute, Emeryville, California, USA

[2]Biological Systems & Engineering Division, Lawrence Berkeley National Laboratory, Berkeley, California, USA

[3]Department of Bioengineering and Biotechnology, Sandia National Laboratory, Livermore, California, USA

[4]Department of Bioengineering, University of California, Berkeley, California, USA

[5]Department of Chemical & Biomolecular Engineering, University of California, Berkeley, California, USA

[6]Novo Nordisk Foundation Center for Biosustainability, Technical University of Denmark, Kogle Alle, DK2970 Hørsholm, Denmark

[*]Corresponding author: Dr. Taek Soon Lee, Joint BioEnergy Institute, 5885 Hollis St. 4th floor, Emeryville, CA 94608, USA; Phone: +1-510-495-2470, Fax: +1-510-495-2629, E-mail: tslee@lbl.gov

Abstract

Inducible gene expression systems are widely used in microbial host strains for protein and commodity chemical production because of their extensive characterization and ease of use. However, some of these systems have disadvantages such as leaky expression, lack of dynamic

[1] Present address: Department of Food Science and Biotechnology, Sungkyunkwan University, Seoul, Republic of Korea

control, and the prohibitively high costs of inducers associated with large-scale production. Quorum sensing (QS) systems in bacteria control gene expression in response to population density, and the LuxI/R system from *Vibrio fischeri* is a well-studied example. A QS system could be ideal for biofuel production strains as it is self-regulated and does not require the addition of inducer compounds, which reduce operational costs for inducer. In this study, a QS system was developed for inducer-free production of the biofuel compound bisabolene from engineered *E. coli*. Seven variants of the Sensor plasmid, which carry the *luxI-luxR* genes, and four variants of the Response plasmid, which carry bisabolene producing pathway genes under the control of the P_{luxI} promoter, were designed for optimization of bisabolene production. Furthermore, a chromosome-integrated QS strain was engineered with the best combination of Sensor and Response plasmid and produced bisabolene at a titer of 1.1 g/L without addition of external inducers. This is a 44% improvement from our previous inducible system. The QS strain also displayed higher homogeneity in gene expression and isoprenoid production compared to an inducible-system strain.

Graphical abstract
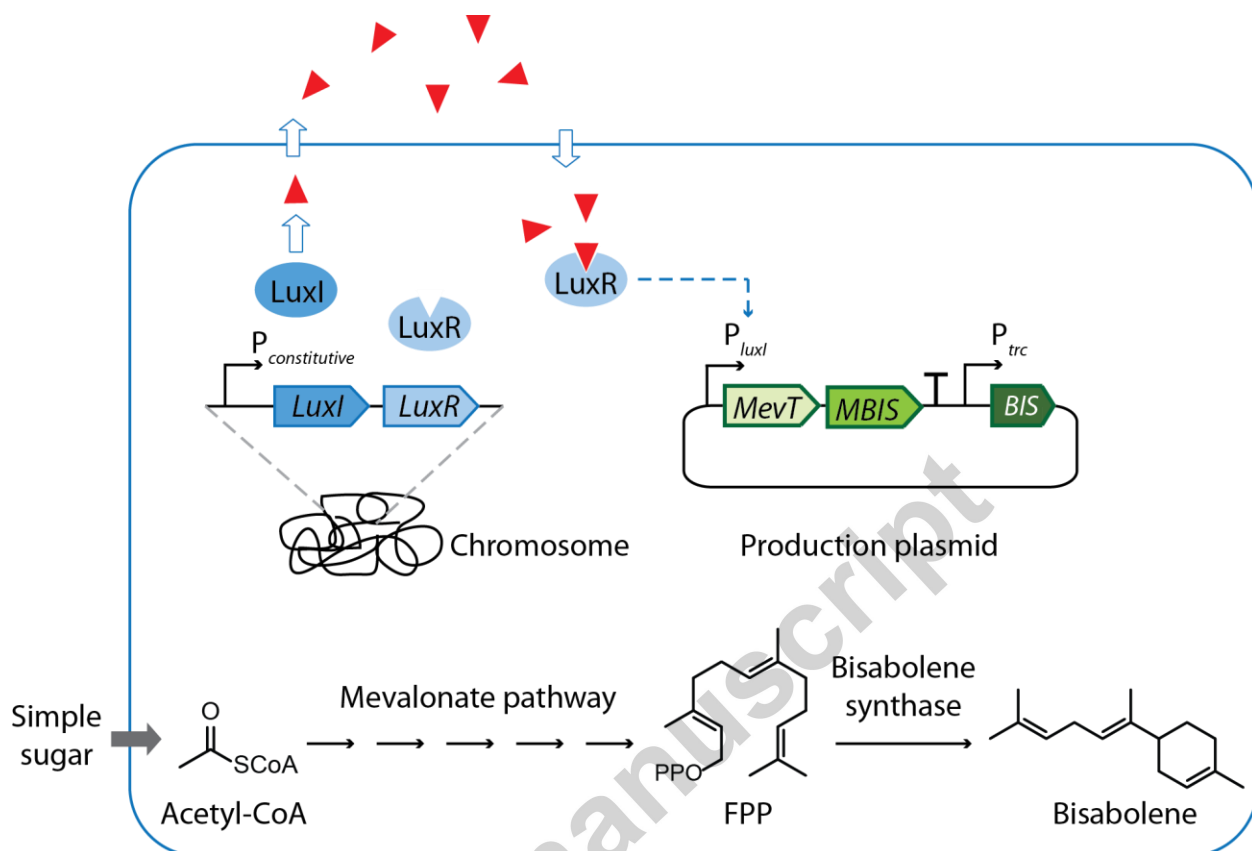
Keywords: quorum sensing (QS), bisabolene, biofuel, synthetic biology, LuxI/R

1. Introduction

Biofuels and bioproducts produced by microbes from lignocellulosic biomass and other renewable feedstocks are a promising alternative to petroleum-derived fuels and chemicals. Biofuel use is associated with a decrease in net greenhouse gas emissions, resulting in less environmental impact compared to petroleum-derived fuels (Antoni et al., 2007; Peralta-Yahya et al., 2012). The production of advanced biofuels representing "drop in" products that can replace petroleum-derived gasoline, diesel, and jet fuel, is a very active field of research (Tian and Lee, 2017). In many cases, these fuels are derived from naturally occurring compounds such as fatty acids and isoprenoids, and have been produced in model organisms such as *Escherichia*

3

coli or *Saccharomyces cerevisiae* through heterologous expression of biosynthetic enzymes (Beller et al., 2015; Buijs et al., 2013; Fortman et al., 2008; Petrovic, 2015).

In biofuel production, inducible promoters have been frequently used to drive gene expression for biosynthesis of various compounds, such as alcohols, short chain alkanes, linear or cyclic isoprenoids, and fatty acid-derived molecules (George et al., 2015; Lee et al., 2008; Liao et al., 2016). There are many advantages in using inducible promoters. For example, one can vary the level of gene expression by varying inducer concentration, and one can also control the timing that the biosynthetic pathway turns on to balance growth and production. However, there are disadvantages of using inducible systems as well, including limited dynamic range, lack of response to cellular state, and most importantly, the cost of the inducer itself (Lee et al., 2011; Saïda et al., 2006; Wang et al., 2015). The use of one of the most popular inducers, isopropyl β-D-1-thiogalactopyranoside (IPTG), is not economically feasible in an industrial setting, where the cost for the required amounts of inducer would be prohibitively high.

One approach to address these drawbacks of using inducible promoters is the use of a dynamic sensor-regulator system to control gene expression in response to the key metabolite in biosynthesis pathways. Previous efforts to develop such sensor-regulator include using acetate sensing protein for lycopene production (Farmer and Liao, 2000), stress-response promoters for amorphadiene synthesis pathway (Dahl et al., 2013), and malonyl-CoA sensing transcription factors for fatty acid biosynthesis in both *E. coli* and yeast (David et al., 2016; Liu et al., 2015; Zhang et al., 2012). These dynamic sensor-regulator systems can efficiently balance cell growth and product synthesis according to cell metabolic state and minimize human supervision (Zhang et al., 2015). However, their use in other pathways and hosts are limited due to the lack of appropriate metabolite-responsive proteins (Holtz and Keasling, 2010). Thus, to extend the

4

autonomous regulation to diverse biosynthesis pathways, a portable, universal autoinduction system should be developed to internally regulate gene expression while balancing biomass production and product synthesis.

In microorganisms, quorum-sensing (QS) is a system that responds to local cell population and triggers expression of genes to synchronize certain behaviors, including antibiotic production, biofilm formation, and virulence (Li et al., 2007; Miller and Bassler, 2001; Wu et al., 2013). QS system has been applied to several biosynthesis pathways to produce glucaric acid, myo-inositol, shikimate (Gupta et al., 2017), β-lactamase exoenzyme (Pai et al., 2012), isopropanol in *E. coli*, and para-hydroxybenzoic acid (PHBA) in *Saccharomyces cerevisiae* (Williams et al., 2015). QS requires two regulatory elements, a signaling molecule (also known as autoinducer) that is constitutively produced and secreted, and a receptor protein that binds the autoinducer and acts as a transcriptional activator of certain genes, including those involved in autoinducer synthesis. Without the autoinducer, the receptor protein is not activated and is unable to promote the expression of the genes under the QS promoter. A well-characterized example of a bacterial QS system is that of *Vibrio fischeri*, involved in luciferase-mediated bioluminescence (Engebrecht et al., 1983). The *V. fischeri* QS system consists of five luciferase structural genes (*luxCDABE*) and two regulatory genes (*luxR* and *luxI*) that mediate quorum sensing. LuxI synthesizes the autoinducer, N-(3-oxohexanoyl)-homoserine lactone (AHL). At a threshold autoinducer concentration, transcription activator, LuxR binds to autoinducer and the LuxR-autoinducer complex activates gene transcription of the *lux* operon promoter (Fuqua et al., 2001; Fuqua et al., 1994).

Recently, a microbial platform for production of bisabolene, a precursor of the biosynthetic alternative to No. 2 diesel (D2) fuel, was developed using a *lac* promoter-based

5

IPTG inducible system (Peralta-Yahya et al., 2011). Although relatively high yield and titer (912 mg/L) of bisabolene was achieved, the commercialization of bisabolene as a diesel fuel using the chemical inducible system may still encounter issues associated with high inducer cost, impeding the competitiveness of biofuels as opposed to conventional diesel fuels. In this study, we developed an external inducer-free gene expression system for bisabolene production via a heterologous mevalonate pathway using the LuxI/R QS system from *V. fischeri* in *E. coli*. This is the first application to establish a fully autonomous QS system for the production of an advanced biofuel, which provides an alternative regulatory approach with no input and no supervision for the biosynthesis of other advanced biofuels.

2. Materials and Methods

All chemicals and media components were purchased from Sigma-Aldrich (St. Louis, MO), Fisher Scientific (Pittsburgh, PA), or VWR (West Chester, PA). *E. coli* DH10B (Invitrogen, Carlsbad, CA) was used for plasmid construction, and DH1 (American Type Culture Collection, Manassas, VA) was used for bisabolene production, since previous study has demonstrated that DH1 strain is more suitable for terpene biosynthesis (Hanahan, 1983; Redding-Johanson et al., 2011).

2.1. Construction of pSensor and pResponse plasmids

All plasmids were derived from the BglBrick plasmid library and constructed using the standard BglBrick cloning method (Anderson et al., 2010; Lee et al., 2011). The pSensor plasmids (pS1-8) were constructed by PCR-amplifying the *luxI* and *luxR* genes from pAC-LuxR/I (pJBEI-6481), digesting with *EcoRI* and *BamHI*, then ligating into pBbS0a, which contains an SC101 replication origin and ampicillin resistance gene. For the pResponse plasmids

6

(pR0-4), pBbA0c- or pBbE0c-P*luxI* vectors were prepared by PCR-amplifying the P*luxI* promoter from pAC-LuxR/I, digesting with *EcoRI* and *BamHI*, and ligating into either pBbA0c or pBbE0c, to provide vectors with a p15A or ColE1 replication origin, respectively. To construct pResponse0 (pR0), monomeric red fluorescent protein (RFP) gene were introduced into pBbA0c-P*luxI* vector by BglBrick Cloning. To construct other pResponse plasmids, various promoter combinations were applied to the top and the bottom portions of the mevalonate pathway. The top portion of the mevalonate pathway, MevT, contains genes for the conversion of acetyl-CoA to mevalonate: acetoacetyl-CoA synthase (*atoB*) from *E. coli*, *E. coli* codon-optimized HMG-CoA synthase (*HMGS*) from *S. cerevisiae* and an *E. coli* codon-optimized and N-terminal-truncated HMG-CoA reductase (*HMGR*) from *S. cerevisiae*. The bottom portion of the mevalonate pathway, MBIS, contains genes for the conversion of mevalonate to farnesyl pyrophosphate (FPP): *E. coli* codon-optimized mevalonate kinase (*MK*) from *S. cerevisiae*, *E. coli* codon-optimized phosphomevalonate kinase (*PMK*) from *S. cerevisiae*, an original phosphomevalonate decarboxylase (*PMD*) from *S. cerevisiae*, IPP isomerase (*idi*) from *E. coli*, and FPP synthase (*ispA*) from *E. coli*. For pR1, the cassette of MevT genes was digested with *BglII*/*XhoI* from pBbA5c-MevT (pJBEI-3100) and ligated into digested pBbA0c-P*luxI* vector to prepare pBbA0c-P*luxI*-MevT. Next, the *BglII*/*XhoI*-digest of pBbS5k-MBIS-T$_{1002}$-P*trc*-Bis (pJBEI-4174) was ligated into the *BamHI*/*XhoI*-digest of pBbA0c-P*luxI*-MevT, generating the final pR1 construct, pBbA0c-P*luxI*-MevT-MBIS-T$_{1002}$-P*trc*-Bis. Plasmids pR2-4 were constructed in a similar fashion to pR1, with the exception that the pR2 and pR4 backbone was prepared using the Golden Gate cloning strategy (Engler et al., 2008),. Inducible production plasmid pBbA5c-MevT-MBIS-T$_{1002}$-P*trc*-Bis (pJBEI-6523) was constructed by ligating the *BamHI*/*XhoI*-

7

digested plasmid pBbA5c-MevT (pJBEI-3100) and *BglII*/*XhoI*-digested plasmid pMBIS-T$_{1002}$-P$_{trc}$-Bis (pJBEI-4174).

2.2. Growth conditions and bisabolene production

The *E. coli*-codon optimized bisabolene synthase from *Abies grandis* was used for bisabolene production as previously described (Peralta-Yahya et al., 2011). For bisabolene production, *E. coli* DH1 was co-transformed with pSensor and pResponse plasmids and cultured as previously described, with the exceptions that cultures were grown in rotary shakers at 200 rpm and 100 μM isopropyl β-D-1-thiogalactopyranoside (IPTG) was added to induce the cells. 8 mL aliquots of induced culture were transferred to culture tubes and overlaid with 10% dodecane. At 24, 48, and 76-hour post-induction, 10 μL of the dodecane layer were sampled and diluted into 990 μL of ethyl acetate spiked with (-)-*trans*-caryophyllene as an internal standard. The samples were analyzed by Agilent 6890 series gas chromatograph (GC) equipped with an Agilent 5973 mass selective (MS) detector and a cyclosyl-B (chiral) capillary column (30 m x 250 mm x 0.25 mm thickness, Agilent) with the following settings: inlet at 250°C, 1.1 mL/min constant flow. The oven was started at 100 °C for 0.75 min, ramped to 250°C at 40°C/min, and held at 250°C for 1 min. The injector and MS quadrupole detector temperatures were 230°C and 150°C, respectively. The MS was operated in selected ion monitoring (SIM) mode using fragment ions of m/z 161, 189, and 204 for bisabolene identification and quantification, as previously described (Anthony et al., 2009; Ozaydin et al., 2013).

2.3. Analysis of pSensor-driven protein expression levels

P$_{luxI}$ promoter strength in pR0 in the presence or absence of a pSensor plasmid was compared to that of pTrc-RFP (pJBEI-2491), pLacUV5-RFP (pJBEI-2488), pConst_S-RFP, pConst_M-RFP and pConst_W-RFP (pJBEI-7534, pJBEI-7535; and, pJBEI-7536) by measuring

RFP expression levels. The constitutive promoters were selected from the Registry of Standard Biological Parts (Ham et al., 2012), with Biobrick part number BBa_J23119, BBa_J23104, and BBa_J23107, respectively. PCR-amplified, and cloned into the pBbA0c vector. Plasmids were transformed into *E. coli* DH1 and cultured in 1 mL EZ-Rich medium with 1% glucose (Teknova, Hollister, CA) in 24-well plates, inoculated at a 1:100 dilution from overnight cultures in LB broth. For strains with inducible promoter, 100 μM IPTG was used. Fluorescence was measured on an Infinite F200 PRO (Tecan, Männedorf, Switzerland) for 30 hours at 30°C, with excitation at 575±10 nm and emission at 620±10 nm. All fluorescence values were normalized to cell density by measuring optical density at 600 nm (OD_{600}).

2.4. Chromosomal integration of pSensor

The kanamycin resistance gene was PCR-amplified from pKD13 with primers P1 and P2 and cloned downstream of the *luxI* and *luxR* genes in both pS2 and pS4 using the standard BglBrick cloning method (Datsenko and Wanner, 2000). Next, each of the *luxI-luxR-kanR* gene sets from pS2 and pS4 were separately PCR-amplified. The amplified gene sets were separately integrated into *E. coli* DH1 using the in-frame single-gene knockout method (Baba et al., 2006) to produce strains JBEI-7581, JBEI-7582, JBEI-7583, and JBEI-7584. Chromosomal integration was verified through colony PCR. Plasmid pR0 was transformed into each host to measure protein expression through RFP fluorescence, as described above. Bisabolene production in the chromosome-integrated QS hosts transformed with separate pResponse plasmids was also measured as described above.

2.5. Population distribution analysis of the biofuel producing hosts with QS system

To confirm the homogeneity of QS-controlled protein expression, monomeric RFP fluorescence in chromosome-integrated QS host (strain JBEI-7581) transformed with pR0 was

compared to that in *E. coli* DH1 transformed with pBbA1c-RFP (inducible system) or DH1 transformed with pS4 and pR0 (strain S4R0, plasmid-QS system). To compare isoprenoid production distribution between inducible and chromosome-QS systems, RFP expression driven by the P$_{rstA}$ promoter, which is responsive to cellular farnesyl pyrophosphate (FPP) levels (Dahl et al., 2013), was measured using flow cytometry. The inducible strain consisted of *E. coli* DH1 transformed with pBbE5c-MBIS and pBbB0a-T$_{1002}$-P$_{rstA}$-RFP and the chromosome-QS strain consisted of JBEI-7581 transformed with pBbE0c-P$_{luxI}$-MBIS and pBbB0a-T$_{1002}$-P$_{rstA}$-RFP. *E. coli* DH1 carrying pBbE0c was used as an empty-vector control. Cultures were grown as described above, supplemented with 5 mM mevalonate, and 100 μM IPTG for the inducible system. Cells were harvested at 10-hour post-induction and stored at -80°C in the presence of 10% glycerol until further analysis. Flow cytometry was performed using a FACSAria II (BD Biosciences, San Jose, CA) equipped with 488-, 561-, and 633-nm solid-state lasers and a forward scatter PMT. A 561 nm (yellow-green) laser was used as the excitation source for RFP fluorescence and emission was collected using a 605/12 filter. Prior to flow cytometry analysis, samples were thawed on ice and diluted 1000-fold to approximately 10^6 cells/mL in PBS. For each sample, 10,000 events were collected at a throughput rate of 800-1200 events/s, using a forward scatter (PMT) threshold of 500. All flow cytometry data were analyzed with the FlowJo package (v. 10.0.6, TreeStar Inc., Ashland, OR). The mean of fluorescence intensity and robust coefficient of variation (rCV) were calculated over all events with a fluorescent intensity higher than 2×10^2 au using the BD Robust Statistics Software. The robust coefficient of variation rCV was calculated as the robust standard deviation divided by the population median, where the robust SD is based upon the deviation of individual data to the median of the population.

10

3. Results

3.1. Initial design of the quorum sensing (QS) system for bisabolene production

To establish a QS-mediated bisabolene pathway in *E. coli*, an initial design platform consisting of two plasmids, pSensor (pS) and pResponse (pR), was implemented (Figure 1). The pSensor plasmid contains the autoinducer synthase (*luxI*) and the regulator (*luxR*) genes from the *V. fischeri*. The pResponse plasmid carries an 8-gene heterologous mevalonate (MVA) pathway for FPP synthesis driven by P_{luxI} promoter, where the top pathway (MevT) contains genes *atoB*, *HMGS*, *HMGR*, and the bottom pathway (MBIS) contains *MK*, *PMK*, *PMD*, *idi*, *ispA* genes. The pResponse plasmid also carries gene *Bis* to convert FPP to bisabolene, driven by a continuously active P_{trc} promoter, as the plasmids and the host strain lack *lacI* gene for the repressor expression. At the threshold level of autoinducer, which accumulates in proportion to cell density, the LuxR-autoinducer complex activates transcription of the P_{luxI} promoter, allowing for bisabolene production through the mevalonate pathway without the addition of external inducer.

To investigate the activity of the designed QS system, pResponse was first constructed using a P_{luxI}-driven RFP gene instead of bisabolene pathway (Figure 1A). The initial sensor plasmid I-pS1 containing gene *luxI/luxR* was constructed on a medium-copy vector with p15A replication origin (pJBEI-7492). The initial response plasmid I-pR0 with gene encoding RFP as a reporter was cloned under P_{luxI} promoter on a low-copy vector with SC101 replication origin (pJBEI-11741) (Figure 2A). In strain I-S1R0, harboring I-pS1 and I-pR0 plasmids (Table 1), the QS system activates RFP expression 11-fold higher than that of strain I-S0R0 harboring I-pR0 and an empty vector I-pS0 (pJBEI-3282), which confirms that the QS system can turn on the target gene expression (Figure 2A). However, we also observed that strain I-S1R0 displayed inconsistent growth rate among its three biological replicates (Figure S2). This abnormal growth

11

behavior may be due to the overproduction of LuxR and LuxI proteins, which may impose metabolic burden and lead to reduced growth and heterogenous cell population.

In the next step, we applied this initial QS system for bisabolene synthesis (Figure 2B). We used the I-pS1 plasmid as our autoinduction system and we constructed a plasmid, I-pR1, with the mevalonate pathway under P$_{luxI}$ promoter, and a bisabolene synthase gene under the constitutive P$_{trc}$ promoter on the low-copy pSC101 vector (pJBEI-7494). To ensure adequate protein expression of the bisabolene synthase, we built another plasmid, I-pS2, by adding an extra copy of *Bis* gene downstream of the *luxR/luxI* gene (pJBEI-7493). By co-transforming the autoinduction plasmid (I-pS1 and I-pS2) and the production plasmid (I-pR1), we built two inducer-free bisabolene producing strains (strains I-QS1 and I-QS2). However, the bisabolene titers were approximately 51 and 44 mg/L in I-QS1 and I-QS2 strains respectively, which is 4.1 and 4.8-fold lower than the titers of the previously reported strains using inducible promoters at 48 hours after induction (pJBEI-2997 + pJBEI-3361) (Peralta-Yahya et al., 2011).

The results of low bisabolene titers led us to suspect that one promoter (P$_{luxI}$) may be inefficient to drive the transcription of all 8 genes for the entire mevalonate pathway. Therefore, we inserted an additional promoter, either a constitutively active P$_{lacUV5}$ or a P$_{luxI}$ promoter respectively, upstream of the MBIS genes and constructed two plasmids, pLacUV5-pR1 and pLuxI-pR1 (pJBEI-7496 and pJBEI-7497). We co-transformed those two plasmids individually with I-pS1 and created strain I-QS1P$_{lacUV5}$ and I-QS1P$_{luxI}$, respectively (Supplementary information). However, comparison of bisabolene production in those strains to the original I-QS1 strain did not show significant improvement for bisabolene production (Supplementary Figure S1). In addition to the lower production titer, we also observed much lower mevalonate pathway protein levels of both the I-QS1 and I-QS2 than the previously reported bisabolene

12

production strain (*E. coli* DH1 harboring pJBEI-2997 and pJBEI-3361) (data not included) (Peralta-Yahya et al., 2011). Hence, based on these observations, we postulated that further optimization of the current QS system is necessary to improve bisabolene production.

3.2. Systematic engineering and characterization of pSensor and pResponse plasmids

The poor protein expression level and bisabolene titer of the initial QS strains suggested that the low-copy production plasmid may be inadequate for bisabolene biosynthesis. In the next step, we employed medium- and high-copy vectors (p15A and ColE1 replication origin, respectively) as pResponse plasmids for the expression of the mevalonate pathway and bisabolene synthase, and a compatible low-copy plasmid (SC101 replication origin) for the autoinduction system (pSensor). To evaluate our modified QS system, plasmid pS1 was constructed with LuxR/LuxI system on SC101 replication origin (pJBEI-7509), and plasmid pR0 was constructed with RFP reporter gene under P$_{luxI}$ promoter on p15A origin (pJBEI-7533). Strain S1R0 bearing plasmid pR0 and pS1 showed 5-fold higher RFP fluorescence (Figure 3) compared to strain S0R0 bearing pR0 and an empty vector pS0 (pJBEI-3276). This result demonstrates that the modified QS system was still able to autonomously activate target gene expression, but the response signal was lower with respect to our initial design (I-S1R0). Additionally, in contrast to strain I-S1R0, we observed consistent growth behavior among the biological replicates of strain S1R0 (Figure S2), which suggested that the deviation in growth rate possibly caused by overexpression of LuxR and LuxI protein may be relieved via using the lower copy of pSensor plasmid. We also compared P$_{luxI}$ promoter strength in S1R0 strain with constitutively active P$_{lacUV5}$ and P$_{trc}$ promoters, which are commonly used to transcribe biosynthesis pathways. We measured RFP fluorescence driven by each promoter, and found that fluorescence in strain S1R0 was about 2-fold lower than that of promoter P$_{lacUV5}$, and 3-fold

13

lower than P*trc*, which indicates that further optimization of this QS system may be needed to enhance the strength of P*luxI* promoter for driving the bisabolene synthesis pathway.

To enhance the response signal of our modified QS system, we sought to improve the activation ability of pSensor plasmids by engineering the promoters of *luxI* and *luxR* genes. In addition to pS1, we constructed 6 additional pSensor variants where constitutive promoters with different strengths (strong: P*const_S*, medium: P*const_M*, and weak: P*const_W*) were used for *luxI* and *luxR* genes (Figure 4A). Variants pS2, pS3, and pS5 containing P*const_S*, P*const_M*, and P*const_W* respectively, were designed in a fashion that one promoter controls transcription of both *luxI* and *luxR*. For variants pS4, pS6, and pS7, on the other hand, *luxR* is controlled by a separate promoter which is stronger than that for *luxI* with a presumption that more LuxR protein is beneficial in activating target genes upon binding to the autoinducer. The relative strengths of the promoter P*const_S*, P*const_M*, P*const_W* were also compared to P*luxI* in strain S1R0 and S0R0 by measuring RFP expression driven by each respective promoter (Figure 4B and Figure S3). As expected, P*const_S* rendered the highest fluorescence signal. Both P*const_S* and P*const_M* promoters are stronger than the activated P*luxI* promoter in S1R0. P*const_W* displayed the lowest fluorescence comparable to the control strain S0R0, where P*luxI* promoter was inactive in the absence of *luxI/luxR* genes.

We co-transformed each pSensor variant with pR0 plasmid, and examined the response signal of those strains by measuring the corresponding RFP expression (Figure 4C, 4E). With different pSensor variants, QS strains generated various response signals. Intriguingly, the RFP response signal seemed highly sensitive to *luxI* gene expression level. By using stronger promoter P*const_M* and P*const_S* to control *luxI* expression, strain S2R0, S3R0 and S4R0 showed improved RFP response signal than strain S1R0. The RFP fluorescence in S2R0 was 15-fold

14

higher, while in strain S3R0 and S4R0, was 23-fold higher than that of strain S1R0. In contrast, RFP fluorescence in strains S5R0, S6R0 and S7R0 were as low as to that of control strain S0R0, due to the use of weak promoter P_{const_W} for *luxI* gene expression. These results suggested that in general, higher *luxI* gene expression level leads to increased activation efficiency of P_{luxI} promoter. The relatively lower response signal of pS2 sensor may result from excessively expressed LuxR and LuxI proteins both under control of P_{const_S} promoter, which may exert unexpected metabolic burden to the cell, leading to impeded expression of RFP gene.

We did not observe a significant correlation between RFP response signal and *luxR* gene expression level from this set of experiment. In strains S5R0, S6R0 and S7R0, *luxI* gene expressions were driven by weak promoter P_{const_W}, while *luxR* expression was driven by strong, medium, and weak promoters (P_{const_S}, P_{const_M}, and P_{const_W}, respectively). Consequently, all three strains S5R0, S6R0 and S7R0 showed similarly low level of RFP fluorescence in spite of changing LuxR expression level. However, this failing of induction of RFP signal may be due to insufficient expression of LuxI protein, which may lessen the effect of changing LuxR protein production. Thus, to fully understand the impact of *luxR* gene expression on pSensor's activation efficiency, a more comprehensive design of experiment is required for future investigation, in which variants with strong and medium *luxI* gene expression combined with strong, medium, and weak *luxR* gene expression will be constructed and characterized.

To compare the autoinduction rates of pSensor variants, it was important we determine the cell density corresponding to the time that RFP fluorescence started to increase. Before autoinduction, cells maintained basal levels of RFP fluorescence among pSensor variants (Figure 4E). After the cell population reached to a threshold, we noticed that RFP fluorescence per cell rapidly increased, generally with a rate of more than 30% per hour. Thus, we denoted the cell

15

density when RFP fluorescence per cell increased by more than 30% per hour as the "switching" OD. Depending on different factors such as the interval time between fluorescence measurements and culture conditions, the switching OD can be different from case to case. Basically, it represents the number of cells that can produce enough autoinducer to turn on the expression of target genes. Therefore, we speculated that the higher expression level of autoinducer synthase in the cell, the lower number of cells are required for activation of target genes. Consistent with our hypothesis, we observed strong positive correlation between the switching OD and *luxI* gene expression level (Figure 4D). When weak promoter was used for LuxI protein synthesis in pSensor variants (i.e. pS5, pS6, and pS7), high switching OD (0.53-0.55) was required for inducing RFP expression. On the other hand, when relatively strong promoters (P$_{const\_M}$ and P$_{const\_S}$) were used in pS2, pS3 and pS4 sensor systems, RFP gene could be activated at low cell density (OD: 0.1-0.12). Finally, when natural P$_{luxI}$ promoter was used for *luxI* expression, medium OD (0.29) was needed for RFP induction.

3.3. Bisabolene production in optimized QS strains

In the previous experiment, we managed to construct seven QS systems with a wide range of P$_{luxI}$ promoter strengths, which could be further used to vary the target MevT and MBIS gene expression and optimize the bisabolene production pathway. To investigate the effect of different QS systems on bisabolene production, we constructed 4 production plasmids, namely pR1, pR2, pR3, pR4 (Figure 5), where the mevalonate pathway genes were controlled by P$_{luxI}$ promoter and *Bis* gene was transcribed by the constitutively active P$_{trc}$ promoter. A medium-copy-number origin (p15A) is used for pR1 and pR2, while a high-copy-number origin (ColE1) was used for pR3 and pR4. For pR1 and pR3 plasmids, MevT and MBIS genes were transcribed by one P$_{luxI}$ promoter. For pR2 and pR4 plasmid, an additional P$_{luxI}$ promoter was inserted

16

upstream of MBIS operon to increase transcription of the bottom mevalonate pathway. To identify the QS system for highest bisabolene production, a combinatorial approach was employed and 28 strains were generated by combining 7 pSensor plasmids and 4 production plasmids (Table 1, pS1-pS7 x pR1-pR4). Bisabolene titers were measured at 24 hours and 72 hours after inoculation. The highest titer, was obtained from strain S3R3 (633.7 mg/L) and S4R4 (633.4 mg/L) after 72 hours as a consequence of combined efforts such as using the sensor variants with highest autoinduction efficiency and high-copy production plasmid. Comparing strain S3R3 with the initial production strains (I-QS1 and I-QS2) at 24-hour time point, the bisabolene titer improved by 8 to 11-fold. However, we found no significant correlation between the bisabolene production and activation ability of pSensor variants characterized using RFP. While pS3 sensor exhibited strong induction efficiency, strains containing pS3 does not always produce high titer. For example, strain S3R1 only achieved 118.5 mg/L bisabolene after 72 hours, which is more than 5-fold lower than that of strain S3R3 containing the same pSensor plasmid. On the other hand, although pSensor variants pS5, pS6, pS7 appeared incapable of inducing RFP expression, their production strains produced certain level of bisabolene (Figure 4 and 5). Especially with high-copy production plasmid pR3 and pR4, the bisabolene titer in strains containing pS5, pS6, or pS7 reached 250-500 mg/L. This result indicated that the effect of low activation ability of pSensor variants on bisabolene production can possibly be diminished by using high-copy production plasmid. Also, the characterized activation efficiency of pSensor variants using RFP may not be able to comprehensively reflect the ability of the QS systems in inducing the bisabolene pathway.

3.4 Chromosomal integration of the QS system and bisabolene production

To address the issues of plasmid instability and metabolic burden, as well as to establish a host strain that can be used for other biosynthesis pathways (Silva et al., 2012), we integrated the QS components of pSensor into *E. coli* chromosome to express LuxR/LuxI proteins. This engineering would generate platform host strains that allow autonomous biosynthesis of diverse pathways by simply using a P$_{luxI}$ promoter to drive the target pathway genes. The pS4 sensor was chosen first for chromosomal integration because it led to the highest bisabolene titer of all the pSensor/pResponse combinations we tested. In addition, we also chose pS2 in the second chromosome-integrated strain because it possesses the strongest constitutive promoter among all the pSensor variants and it could compensate the impact of switching the autoinduction system from multi-copy plasmid to single-copy chromosome, even though the autoinduction efficiency, cell growth, and bisabolene production in strains containing pS2 were not as optimal as those in the strains with pS4. Two non-essential genes, *poxB* and *recA*, which respectively encode a pyruvate oxidase and a recombinase, were targeted as loci for replacement by *luxI-luxR* cassettes. In particular, we chose *poxB* locus since the *ΔpoxB* strain was reported to display improved production due to the decrease in acetate accumulation associated with *poxB* mutation or deletion (Dittrich et al., 2005).

We constructed four QS-mediated hosts by replacing either *poxB* or *recA* gene with sensor systems from pS2 or pS4. The activation properties of those QS-integrated hosts were assessed by analyzing RFP expression driven by P$_{luxI}$ promoter (i.e. plasmid pR0) in each host, and compared to the RFP values with their cognate plasmid-borne QS strains (Figure 6A). We found that expression of RFP in strains *ΔpoxB*::pS2 (JBEI-7581) and *ΔrecA*::pS2 (JBEI-7582) was higher or comparable to that in the strain harboring plasmid pS2 (S2R0). However, expression levels in strains *ΔpoxB*::pS4 (JBEI-7583) and *ΔrecA*::pS4 (JBEI-7584) were much

18

lower than those of the pS4 plasmid-borne strain. This low activation ability may be due to the reduced LuxR/LuxI protein expression resulted by changing the QS system from plasmid-borne to genome integrated system.

To test bisabolene production in the QS-integrated hosts, we transformed four production plasmids (pR1, pR2, pR3, pR4) into the *ΔpoxB*::pS2 (JBEI-7581) strain which showed the highest efficiency of autoinduced production. We also constructed two inducible bisabolene production strains C1 and C2 as controls, where C1 consists of plasmids pS0 and pC1 (pJBEI-7527), and C2 consists of plasmids pS0 and pC2 (pJBEI-7528). Plasmid pC1 was constructed based on pR1 where P$_{luxI}$ was replaced by P$_{lacUV5}$ and *lacI* gene was added to confer inducible expression of the pathway. Similarly, plasmid pC2 was constructed based on pR2, where the P$_{luxI}$ promoter upstream of MVA operon was replaced by P$_{lacUV5}$, the other P$_{luxI}$ promoter upstream of MBIS operon was replaced by P$_{trc}$, meanwhile, *lacI* gene was also added, so all promoters are controlled by inducers. The plasmid architecture and operon organization of pC1 and pC2 resembles that of response plasmid pR1 and pR2 respectively. By comparing C1 and C2 with QS integrated hosts containing pR1 and pR2, we sought to explore the alternatives of using QS autoinduction system instead of inducible promoters for bisabolene production while generating equal or higher titer and productivity.

Bisabolene productions at 24, 48, and 72-hour post inoculation were measured for the QS-mediated hosts and control plasmids (Figure 6B). We found that strains C1 and C2 produced 327.1 mg/L and 771.2 mg/L bisabolene, respectively after 72 hours. In contrast, QS hosts containing pR1 and pR2 reached 465.3 mg/L and 253.6 mg/L bisabolene titer, which is 42% higher than strain C1 and 67% lower than strain C2. Surprisingly, QS strains with higher copy number pResponse plasmids (pR3, pR4) did not show improved production than strains bearing

19

pR1 and pR2. Moreover, the highest titer among the QS strains only reached 470.8 mg/L from hosts containing pR4, which is 39% lower than C2 strain and 26% lower than the highest titer obtained from plasmid-borne QS strain S4R4. These results led us to speculate that the pathway may need further optimization for the QS-integrated host as it contains a new genetic context that differs from the plasmid-borne system. Since it has been previously reported that enzymes in MevT operon were expressed at considerably higher levels than those in MBIS operon on the same plasmid, the high MevT enzyme expression and inadequate MBIS enzyme production may then cause mevalonate accumulation which inhibits MK activity (Ma et al., 2011). Therefore, we redesigned the bisabolene pathway into two plasmids, a low-copy plasmid for MevT operon (pJBEI-7554) and a medium-copy plasmid for MBIS operon and *Bis* genes (pJBEI-7555). We transformed those two plasmids into the QS-integrated hosts and created strains *ΔrecA*::pS2-SA and *ΔpoxB*::pS2-SA (Table 1). We found that bisabolene production of these strains reached 1.1 g/L, which is 44% higher than that of control strain C2 (Figure 6C). This result is a significant improvement in bisabolene production, and establishes pS2 integrated QS host strain as a useful platform that can be generally used for other biofuel pathways and industrial applications.

3.5 Population distribution of producing cells with QS system

Due to the inherent stochastic nature of biological processes, non-genetic, cell-to-cell variations in protein expression and metabolite synthesis often give rise to subpopulations of both low- and high-producing variants in microbial culture (Papenfort and Bassler, 2016). Historically, the QS autoinduction system has been considered a critical factor to small genetic variations since it synchronizes stochastic biological events among individual cells in an isogenic population (Davidson and Surette, 2008). To examine the population variation of QS-mediated system in comparison to the inducible system, flow cytometry was used to determine protein

20

expression homogeneity as it allows for measurements at the single-cell level. Using RFP as a reporter, we compared the mean fluorescence intensity and fluorescence distribution among three strains: QS integrated strain containing pR0 in *ΔpoxB*::pS2 host, S4R0 as QS plasmid-borne strain and inducible strain containing P*trc*-driven RFP. The robust coefficient of variation (rCV) was used to measure the level of population spread (Hoffman and Wood, 2007), which is more resistant to the statistical influences of outlying events in a sample population compared to classical CV (Figure 7A). We found that at 10 hours after induction, fluorescence of each system was narrowly distributed with mean fluorescence levels of 6607, 11313, and 5619 au, and rCV values of 72%, 56.1%, and 57.8% for inducible, QS plasmid and QS integrated systems (Figure 7B and C), respectively. The rCV values associated with both QS systems are smaller than the inducible system, suggesting the improved population homogeneity for QS-mediated protein expression system. However, we did observe a second peak with lower fluorescence in all three systems, accounting for 2-7% of the populations (4.2% for inducible strain, 7.2% for chromosomally integrated QS strain, and 2% for plasmid-based QS strain). This observation implies that QS-dependent protein expression could also display small genetic variations, and the plasmid-borne QS system may confer the highest population homogeneity among all three systems.

    Not only did we explore the homogeneity of protein expression, we also sought to compare the population variation of metabolite-producing cells among these three systems. Since FPP is the key intermediate metabolite in our pathway, we measured the degree of homogeneity of cells bearing genes encoding the mevalonate pathway. To link the FPP production variation to fluorescence variation that could be detected by flowcytometry, we took advantage of a previously discovered FPP-sensor, promoter P*rstA*, whose strength was reported to be

proportional to the intracellular FPP concentration (Dahl et al., 2013). Thus, in the presence of FPP biosynthesis pathway, the intensity of P_{rstA}-driven RFP can reflect the intracellular level of FPP, and the spread of the RFP fluorescence distribution can represent the population variation of FPP-producing cells. We constructed a plasmid (pJBEI-7550) containing MBIS genes, which can produce FPP with supplementation of mevalonate, and a second plasmid (pJBEI-7549) containing RFP gene driven by P_{rstA} promoter. For the QS system, P_{luxI} promoter was used to control MBIS genes in strain $\Delta poxB$::pS2 (JBEI-7581), while for the inducible system, P_{lacUV5} was used to induce the MBIS operon. As a control system, we constructed a strain consisting of an empty plasmid vector and a plasmid with P_{rstA}-driven RFP, so the RFP fluorescence was not linked to FPP production (Figure 7D). We observed comparable fluorescence intensity between the inducible and QS systems, with mean fluorescence intensities of 5642 vs. 4909 au, respectively, indicating similar FPP production levels for both strains. In terms of population variation, we found that the QS system showed higher homogeneity with less spread (or a lower rCV among all three strains), suggesting that the QS system endows higher level of coordinated multi-cellular behaviors in FPP-producing strains (Figure 7F). However, with the addition of FPP-synthesis pathway, the non-fluorescent peak also became more pronounced in both systems, accounting for 8.8% and 9.9% of the inducible and QS populations, respectively, which is most likely due to toxicity and metabolic burden generated by FPP biosynthesis.

4. Discussion

Previous work has shown that QS systems can be tuned to achieve various activation properties including the autoinduction time, OD, and strength of response signal. Consequently, there's a trade-off between obtaining high activation efficiency and increasing biomass

22

production. Higher LuxI protein production leads to efficient activation of target genes, but the switching point shifts at earlier growth time and lower OD, thus conferring metabolic burden and reduced cell growth. On the other hand, weaker LuxI protein expression level results in lower activation efficiency and response signal, but higher "switching" OD since more cells are required to reach the threshold intracellular autoinducer concentration for triggering QS response, thus achieving higher biomass production (Gupta et al., 2017; Pai et al., 2012). In agreement with these findings, similar phenomenon was observed during the characterization of seven pSensor variants as shown in Figure 4. In general, a high RFP response signal at a low switching OD were obtained from pS2, pS3 and pS4 sensors, where relatively strong promoters (P$_{const\_M}$, P$_{const\_S}$) were used to control *luxI* gene. Medium induction strength and OD were obtained from pSensor pS1 with P$_{luxI}$-driven *luxI* gene, while low RFP and high switching OD were obtained from pS5, pS6 and pS7 by using weak promoter to control *luxI* gene.

One of the most notable results of our work is that we demonstrated QS-mediated system imparts higher homogeneity for not only single protein expression (such as RFP) but also metabolite production via metabolic pathway than chemical-inducible system. Many examples have used flow cytometric analyses to measure signal distribution of single gene response to QS systems (Grote et al., 2015). However, few has been reported that measures the population variation associated with QS-mediated metabolic pathway. Here, we investigated the homogeneity of FPP-producing strains by connecting the biosynthesis pathway to RFP. We used an FPP-sensor promoter P$_{rstA}$ to drive RFP expression, thus, converting the FPP production variation to fluorescence distribution that can be further quantified by flowcytometry. As FPP is an essential intermediate metabolite in isoprenoid pathway, our finding can potentially provide

23

insights into a variety of isoprenoid-derived chemical production using quorum-sensing induction strategy.

Quorum-sensing is a ubiquitous phenomenon in microorganisms that regulates diverse phenotypic behaviors. A variety of microorganisms were identified with QS system including *Staphylococcus sp., Pseudomonas sp, C. glutamicum*, and others (Miller and Bassler, 2001; Papenfort and Bassler, 2016). Due to the recent advances in synthetic biology and metabolic engineering, multiple QS systems have been applied for biosynthesis pathway optimization. For example, a QS-linked RNA interference system was developed for dynamic pathway control to produce *p*-hydroxybenzoic acid (PHBA) in *Saccharomyces cerevisiae* (Williams et al., 2015). A QS system capable of down-regulating target protein expression from *Pantoea stewartii* subsp. was employed to produce glucaric acid in *E. coli* (Gupta et al., 2017) Recently, a QS-mediated system from *V. fischeri* has also been used to develop a toggle switch for redirecting metabolic flux from TCA cycle to isopropanol synthesis (Soma and Hanai, 2015). This study established a design method to use QS system for controlling biofuel production, however, the QS system still requires external IPTG inducer to turn on LuxR/LuxI expression as well as the isopropanol pathway, which therefore, only accomplished semi-autonomous regulation of the pathway biosynthesis. In contrast, our study focused on developing a fully self-induced system that requires no inducer and no human supervision. We achieved high bisabolene production using our QS platform, which demonstrated that this system has the potential to be applied to industry for commercialization of biofuel production.

5. Conclusion

In this study, inducer-free bisabolene production was achieved by expressing LuxR/LuxI effector-regulator proteins and using P$_{luxI}$ responsive promoter to drive target biosynthesis pathway. By engineering promoters of LuxR/LuxI proteins, seven variants of pSensor plasmids were designed with diverse autoinduction efficiency. Four pResponse plasmids carrying bisabolene synthesis pathway were co-transformed with the seven pSensor plasmids, generating a library of 28 self-inducing bisabolene production strains. The best performer achieved 633 mg/L bisabolene production after 72 hours. In addition, to address the issues associated with plasmid stability and to reduce the metabolic burden of plasmid-bearing strains, the QS sensor was integrated into *E. coli* genome to develop QS-mediated host for a broad range of biosynthesis pathways. Using this host, production of bisabolene further improved to 1.1 g/L, which is 44% of theoretical yield via the MVA pathway (0.25 g/g glucose). From our study, we show that QS provides a promising approach for biofuels production without external inducer addition and human supervision, which can significantly reduce material and labor cost for biofuel commercialization.

Acknowledgements

References

Anderson, J. C., Dueber, J. E., Leguia, M., Wu, G. C., Goler, J. A., Arkin, A. P., Keasling, J. D., 2010. BglBricks: A flexible standard for biological part assembly. J Biol Eng. 4**,** 1-12.

Anthony, J. R., Anthony, L. C., Nowroozi, F., Kwon, G., Newman, J. D., Keasling, J. D., 2009. Optimization of the mevalonate-based isoprenoid biosynthetic pathway in Escherichia coli for production of the anti-malarial drug precursor amorpha-4,11-diene. Metab Eng. 11, 13-19.

Antoni, D., Zverlov, V. V., Schwarz, W. H., 2007. Biofuels from microbes. Appl Microbiol Biotechnol. 77, 23-35.

Baba, T., Ara, T., Hasegawa, M., Takai, Y., Okumura, Y., Baba, M., Datsenko, K. A., Tomita, M., Wanner, B. L., Mori, H., 2006. Construction of Escherichia coli K-12 in-frame, single-gene knockout mutants: the Keio collection. Mol Syst Biol. 2, 1-11.

Beller, H. R., Lee, T. S., Katz, L., 2015. Natural products as biofuels and bio-based chemicals: fatty acids and isoprenoids. Nat Prod Rep. 32, 1508-1526.

Buijs, N. A., Siewers, V., Nielsen, J., 2013. Advanced biofuel production by the yeast Saccharomyces cerevisiae. Curr Opin Chem Biol. 17, 480-488.

Dahl, R. H., Zhang, F., Alonso-Gutierrez, J., Baidoo, E., Batth, T. S., Redding-Johanson, A. M., Petzold, C. J., Mukhopadhyay, A., Lee, T. S., Adams, P. D., Keasling, J. D., 2013. Engineering dynamic pathway regulation using stress-response promoters. Nat Biotechnol. 31, 1039-1046.

Datsenko, K. A., Wanner, B. L., 2000. One-step inactivation of chromosomal genes in Escherichia coli K-12 using PCR products. Proc. Natl. Acad. Sci. USA 97, 6640–6645.

David, F., Nielsen, J., Siewers, V., 2016. Flux Control at the Malonyl-CoA Node through Hierarchical Dynamic Pathway Regulation in Saccharomyces cerevisiae. ACS Synth Biol. 5, 224-233.

Davidson, C. J., Surette, M. G., 2008. Individuality in bacteria. Annu Rev Genet. 42, 253-268.

Dittrich, C. R., Vadali, R. V., Bennett, G. N., San, K. Y., 2005. Redistribution of metabolic fluxes in the central aerobic metabolic pathway of E. coli mutant strains with deletion of the ackA-pta and poxB pathways for the synthesis of isoamyl acetate. Biotechnol Prog. 21**,** 627-631.

Engebrecht, J., Nealson, K., Silverman, M., 1983. Bacterial bioluminescence: Isolation and genetic analysis of functions from Vibrio fischeri. Cell. 32**,** 773-781.

Engler, C., Kandzia, R., Marillonnet, S., 2008. A one pot, one step, precision cloning method with high throughput capability. PLoS One. 3**,** e3647.

Farmer, W. R., Liao, J. C., 2000. Improving lycopene production in Escherichia coli by engineering metabolic control. Nature biotechnology. 18**,** 533-537.

Fortman, J. L., Chhabra, S., Mukhopadhyay, A., Chou, H., Lee, T. S., Steen, E., Keasling, J. D., 2008. Biofuel alternatives to ethanol: pumping the microbial well. Trends Biotechnol. 26**,** 375-381.

Fuqua, C., Parsek, M. R., Greenberg, E. P., 2001. Regulation of gene expression by cell-to-cell communication: acyl-homoserine lactone quorum sensing. Annu Rev Genet. 35**,** 439-468.

Fuqua, W. C., Winans, S. C., Greenberg, E. P., 1994. Quorum sensing in bacteria: the LuxR-LuxI family of cell density-responsive transcriptional regulators. J Bacteriol. . 176**,** 269-275.

George, K. W., Alonso-Gutierrez, J., Keasling, J. D., Lee, T. S., 2015. Isoprenoid drugs, biofuels, and chemicals--artemisinin, farnesene, and beyond. Adv Biochem Eng Biotechnol. 148**,** 355-389.

Grote, J., Krysciak, D., Streit, W. R., 2015. Phenotypic Heterogeneity, a Phenomenon That May Explain Why Quorum Sensing Does Not Always Result in Truly Homogenous Cell Behavior. Appl Environ Microbiol. 81**,** 5280-5289.

Gupta, A., Reizman, I. M., Reisch, C. R., Prather, K. L., 2017. Dynamic regulation of metabolic flux in engineered bacteria using a pathway-independent quorum-sensing circuit. Nat Biotechnol. 35**,** 273-279.

Ham, T. S., Dmytriv, Z., Plahar, H., Chen, J., Hillson, N. J., Keasling, J. D., 2012. Design, implementation and practice of JBEI-ICE: an open source biological part registry platform and tools. Nucleic Acids Res. 40**,** e141.

Hanahan, D., 1983. Studies on transformation of Escherichia coli with plasmids. Journal of molecular biology 166,**,** 557–580.

Hoffman, R. A., Wood, J. C. S., 2007. Characterization of Flow Cytometer Instrument Sensitivity. Current Protocols in Cytometry 1**,** 1-18.

Holtz, W. J., Keasling, J. D., 2010. Engineering static and dynamic control of synthetic pathways. Cell. 140**,** 19-23.

Lee, S. K., Chou, H., Ham, T. S., Lee, T. S., Keasling, J. D., 2008. Metabolic engineering of microorganisms for biofuels production: from bugs to synthetic biology to fuels. Curr Opin Biotechnol. 19**,** 556-563.

Lee, T. S., Rachel A Krupa, R. A., Zhang, F., Hajimorad, M., Holtz, W. J., Prasad, N., Lee, S. K., Keasling, J. D., 2011. BglBrick vectors and datasheets: A synthetic biology platform for gene expression. Journal of Biological Engineering. 5**,** 1-14.

28

Li, J., Attila, C., Wang, L., Wood, T. K., Valdes, J. J., Bentley, W. E., 2007. Quorum sensing in Escherichia coli is signaled by AI-2/LsrR: effects on small RNA and biofilm architecture. J Bacteriol. 189, 6011-20.

Liao, J. C., Mi, L., Pontrelli, S., Luo, S., 2016. Fuelling the future: microbial engineering for the production of sustainable biofuels. Nat Rev Microbiol. 14, 288-304.

Liu, D., Xiao, Y., Evans, B. S., Zhang, F., 2015. Negative feedback regulation of fatty acid production based on a malonyl-CoA sensor-actuator. ACS Synth Biol. 4, 132-140.

Ma, S. M., Garcia, D. E., Redding-Johanson, A. M., Friedland, G. D., Chan, R., Batth, T. S., Haliburton, J. R., Chivian, D., Keasling, J. D., Petzold, C. J., Lee, T. S., Chhabra, S. R., 2011. Optimization of a heterologous mevalonate pathway through the use of variant HMG-CoA reductases. Metab Eng. 13, 588-597.

Miller, M. B., Bassler, B. L., 2001. Quorum sensing in bacteria. Annu Rev Microbiol. 55, 165–199.

Ozaydin, B., Burd, H., Lee, T. S., Keasling, J. D., 2013. Carotenoid-based phenotypic screen of the yeast deletion collection reveals new genes with roles in isoprenoid production. Metab Eng. 15, 174-183.

Pai, A., Tanouchi, Y., Youa, L., 2012. Optimality and robustness in quorum sensing (QS)mediated regulation of a costly public good enzyme. PNAS. 109, 19810–19815.

Papenfort, K., Bassler, B. L., 2016. Quorum sensing signal-response systems in Gram-negative bacteria. Nat Rev Microbiol. 14, 576-588.

Peralta-Yahya, P. P., Ouellet, M., Chan, R., Mukhopadhyay, A., Keasling, J. D., Lee, T. S., 2011. Identification and microbial production of a terpene-based advanced biofuel. Nat Commun. 2, 1-8.

29

Peralta-Yahya, P. P., Zhang, F., del Cardayre, S. B., Keasling, J. D., 2012. Microbial engineering for the production of advanced biofuels. Nature. 488**,** 320-328.

Petrovic, U., 2015. Next-generation biofuels: a new challenge for yeast. Yeast. 32**,** 583-93.

Redding-Johanson, A. M., Batth, T. S., Chan, R., Krupa, R., Szmidt, H. L., Adams, P. D., Keasling, J. D., Lee, T. S., Mukhopadhyay, A., Petzold, C. J., 2011. Targeted proteomics for metabolic pathway optimization: application to terpene production. Metab Eng. 13**,** 194-203.

Saïda, F., Uzan, M., B., O., Bontems, F., 2006. Expression of Highly Toxic Genes in E. coli: Special Strategies and Genetic Tools. urrent Protein and Peptide Science. 7**,** 7, 47-56.

Silva, F., Queiroz, J. A., Domingues, F. C., 2012. Evaluating metabolic stress and plasmid stability in plasmid DNA production by Escherichia coli. Biotechnol Adv. 30**,** 691-708.

Soma, Y., Hanai, T., 2015. Self-induced metabolic state switching by a tunable cell density sensor for microbial isopropanol production. Metab Eng. 30**,** 7-15.

Tian, T., Lee, T. S., 2017. Advanced Biodiesel and Biojet Fuels from Lignocellulosic Biomass. 1-25.

Wang, B., Barahona, M., Buck, M., 2015. Amplification of small molecule-inducible gene expression via tuning of intracellular receptor densities. Nucleic Acids Res. 43**,** 1955-1964.

Williams, T. C., Averesch, N. J., Winter, G., Plan, M. R., Vickers, C. E., Nielsen, L. K., Kromer, J. O., 2015. Quorum-sensing linked RNA interference for dynamic metabolic pathway control in Saccharomyces cerevisiae. Metab Eng. 29**,** 124-134.

Wu, H. C., Tsao, C. Y., Quan, D. N., Cheng, Y., Servinsky, M. D., Carter, K. K., Jee, K. J., Terrell, J. L., Zargar, A., Rubloff, G. W., Payne, G. F., Valdes, J. J., Bentley, W. E.,

2013. Autonomous bacterial localization and gene expression based on nearby cell

receptor density. Mol Syst Biol. 9**,** 636.

Zhang, F., Carothers, J. M., Keasling, J. D., 2012. Design of a dynamic sensor-regulator system

for production of chemicals and fuels derived from fatty acids. Nat Biotechnol. 30**,** 354-

359.

Zhang, J., Jensen, M. K., Keasling, J. D., 2015. Development of biosensors and their application

in metabolic engineering. Curr Opin Chem Biol. 28**,** 1-8.

List of Figures

Figure 1
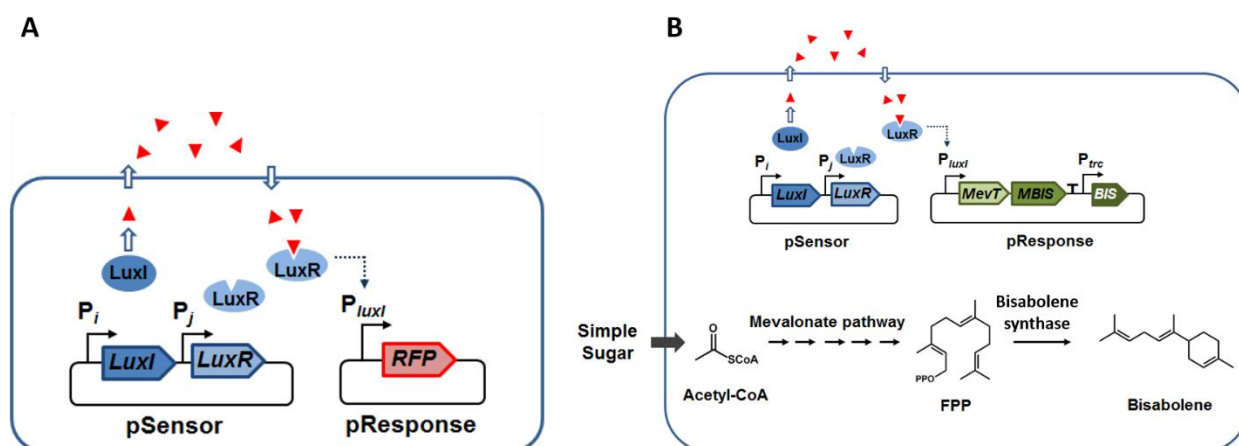
Figure 1. Implementation of quorum sensing (QS) system to bisabolene production. (A) pSensor plasmid and pResponse plasmid were constructed to evaluate the induction efficiency of quorum-sensing system. pSensor plasmid consists of gene *luxI* and *luxR,* which are controlled by promoter P_i and P_j. LuxI protein synthesizes autoinducer N-(3-oxohexanoyl)-homoserine lactone (triangle), which can diffuse in or out of neighboring cells and binds to LuxR protein. pResponse plasmid consists of RFP reporter gene driven by promoter P_{luxI}. At a threshold concentration of autoinducer, the autoinducer-bound LuxR protein activates P_{luxI} promoter and induces RFP expression. P_i and P_j denote either the native P_{luxI} and P_{luxR} promoters in our initial designs or the synthetic constitutive promoters in our later experiments. **(B)** pResponse plasmid consists of mevalonate pathway (*MevT* and *MBIS* genes) driven by P_{luxI} promoter and bisabolene synthase (*BIS* gene) driven by a constitutively expressed P_{trc} promoter. At a threshold concentration of autoinducer, the autoinducer-bound LuxR protein activates P_{luxI} promoter and induce the mevalonate pathway.
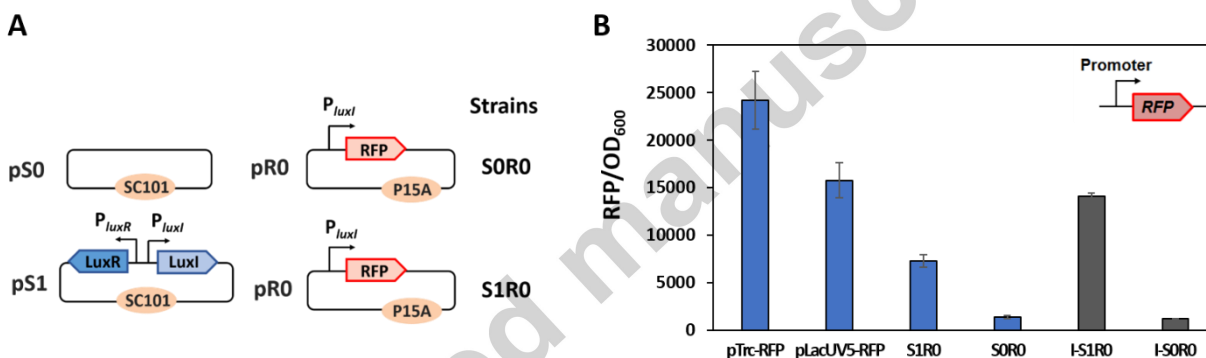
Figure 2
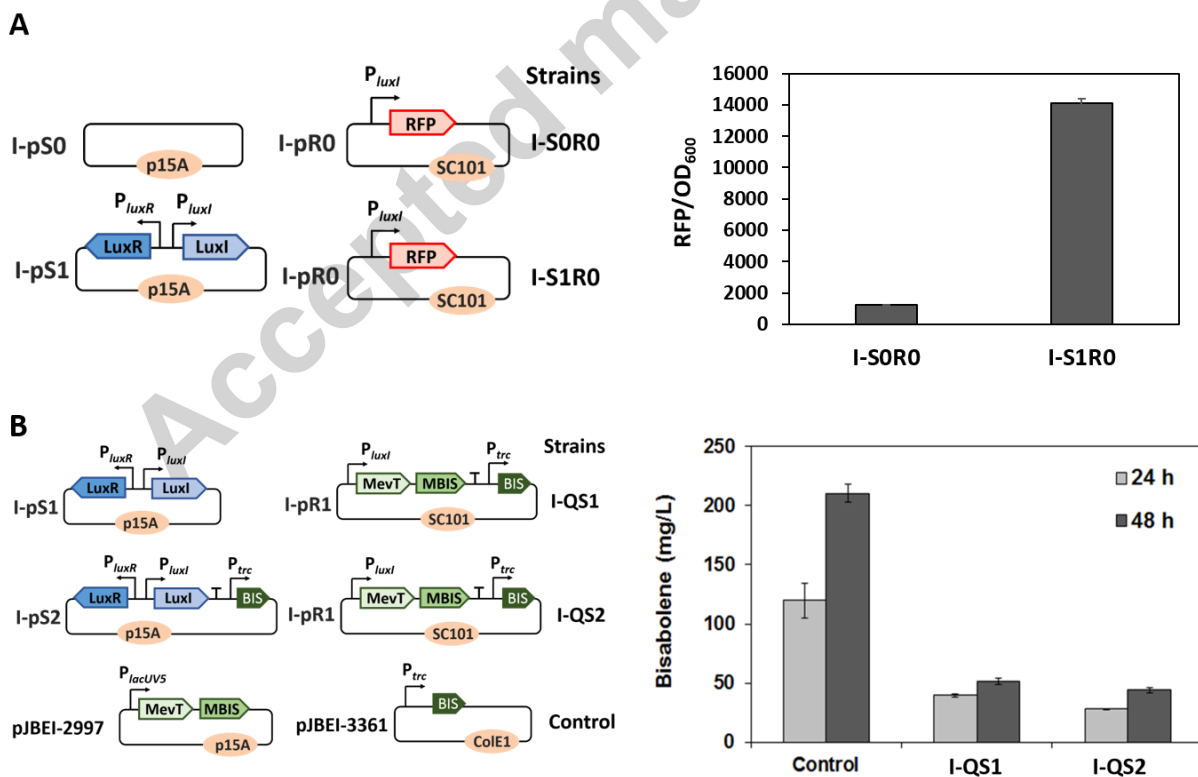
Figure 2. Initial design platform of the QS-mediated bisabolene production system. pSensor plasmid has p15A replication origin and pResponse plasmid has SC101 replication

origin. **(A)** Activation of RFP protein expression by QS system in strain I-S1R0 compared to I-S0R0. Left: Plasmid architecture of strain I-S1R0 and I-S0R0. Right: RFP response signal in strain I-S0R0 and I-S1R0. Plasmid I-pS0 is an empty vector; plasmid I-pS1 contains *luxR* gene driven by native P_{luxR} and *luxI* gene driven by P_{luxI} promoter; plasmid I-pR0 consists of RFP gene driven by P_{luxI} promoter. **(B)** Bisabolene production of strain I-QS1 and I-QS2. Left: Plasmid architecture of strain I-QS1, I-QS2 and the control strain. Plasmid I-pR1 contains mevalonate pathway driven by P_{luxI} promoter and bisabolene synthase gene (*BIS*) driven by constitutively expressed P_{trc} promoter; plasmid I-pS2 contains *BIS* gene in addition to *luxI/luxR* genes, which is also driven by a constitutively expressed P_{trc} promoter. Plasmids pJBEI-2997 and pJBEI-3361 were transformed into *E. coli* DH1to prepare a control strain. Right: Bisabolene production after 24 hours and 48 hours. Error bar represents data from biological triplicates.
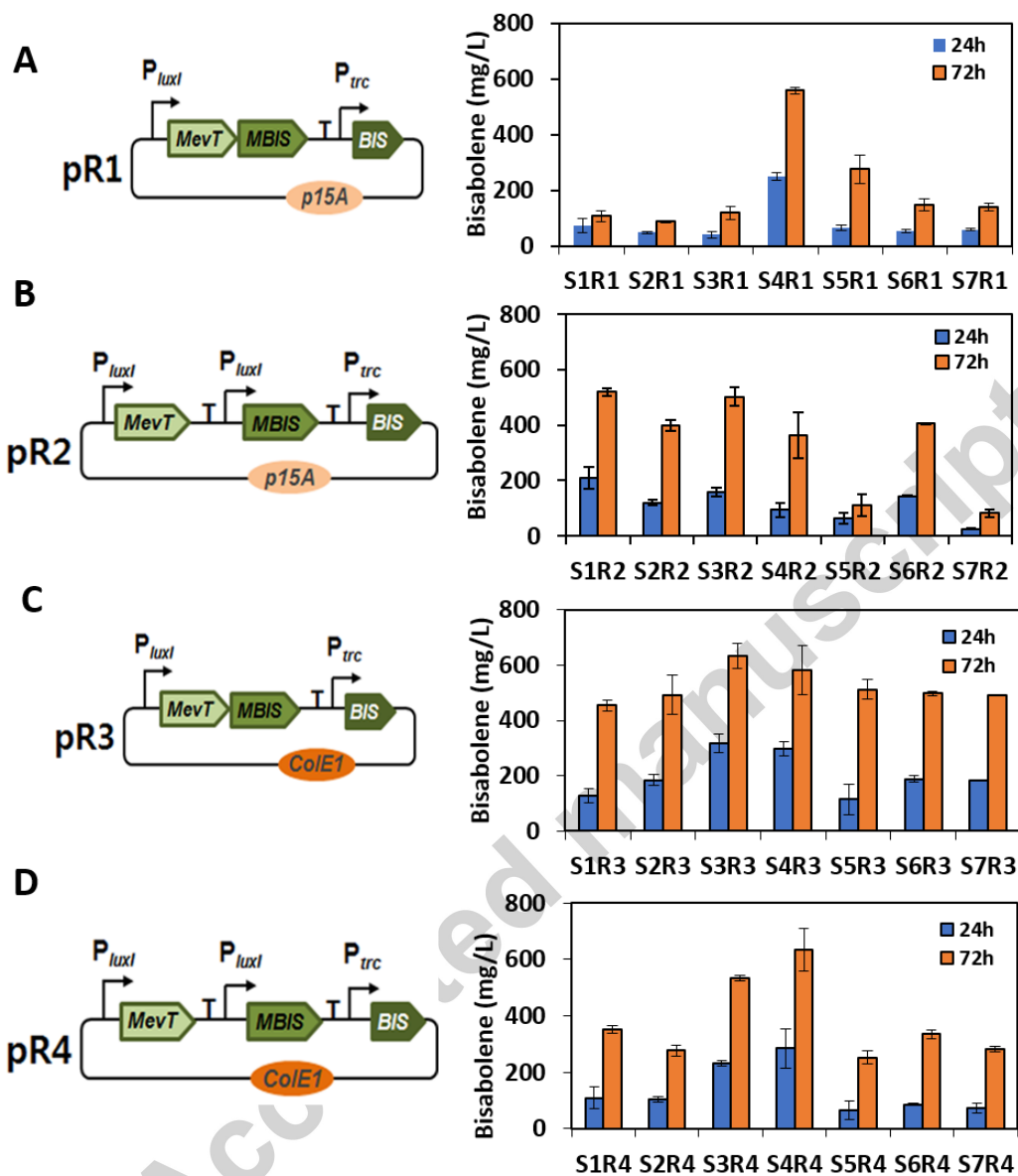
Figure 3

Figure 3. Activation properties of the modified QS system. In the modified QS system, pSensor plasmid has SC101 replication origin and pResponse plasmid has p15A origin. **(A)** plasmid architecture in strain S0R0 and S1R0.Plasmid pS0 is an empty vector; plasmid pS1 contains *luxR* gene driven by native P_{luxR} and *luxI* gene driven by P_{luxI} promoter; plasmid pR0 consists of RFP gene driven by P_{luxI} promoter. **(B)** RFP response signal in the modified QS strain S1R0 compared to strain S0R0 and strain harboring constitutively expressed RFP driven by promoter P_{trc} and P_{lacUV5}. As a control, RFP expression in initial QS strain I-S1R0 and I-S0R0 were also shown in grey color. In strains I-S1R0 and I-S0R0, the RFP reporter is on low copy plasmid with SC101 origin, while in strains S1R0 and S0R0, the RFP reporter is on medium copy plasmid with P15A origin.
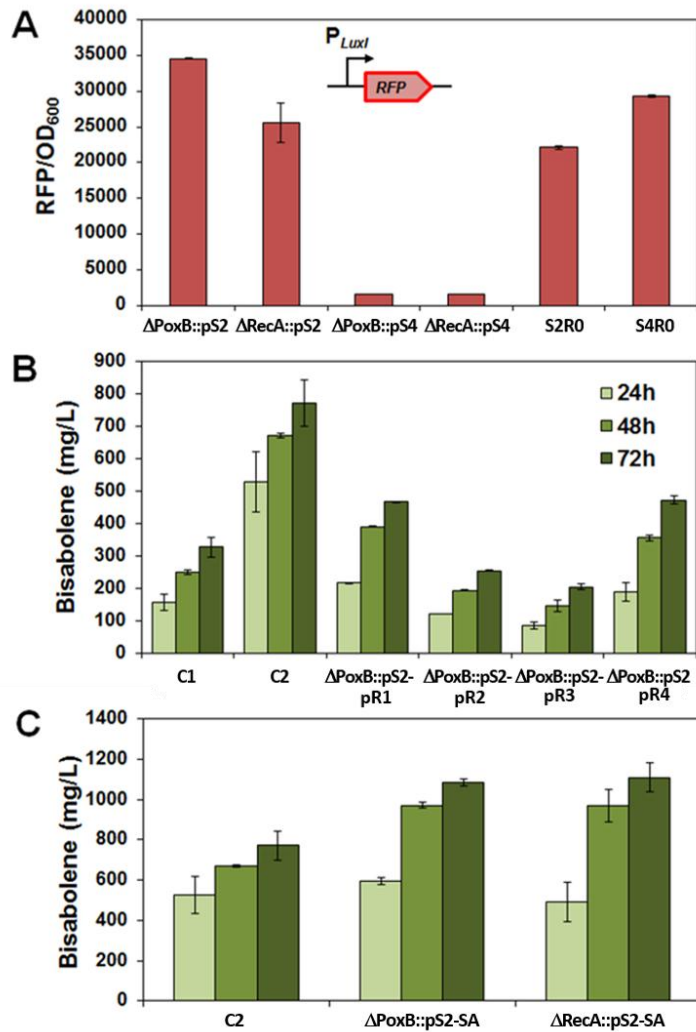
Figure 4
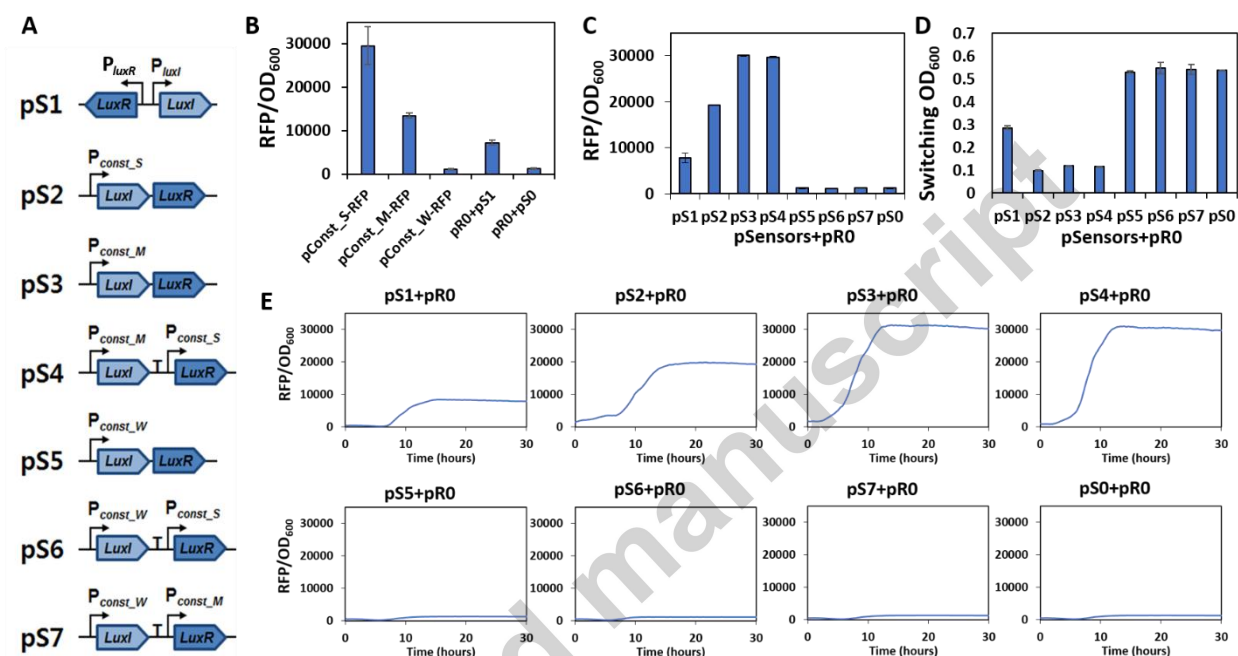
Figure 4. Construction and characterization of QS sensor variants. pR0 plasmid containing RFP reporter gene was co-transformed with each pSensor variant during the characterization. **(A)** Schematics of pSensor variants with different constitutive promoters. **(B)** Comparison of promoter strength between constitutive promoters P_{const_S}, P_{const_M}, P_{const_W} and P_{luxI} promoter in S0R0 and S1R0 strains. **(C)** End point RFP activation signal among pSensor variants. **(D)** Cell density (OD_{600}) of the time that RFP was activated among seven pSensor variants. **(E)** Time-course RFP activation signal among pSensor variants. The P_{luxR} promoter region is poorly defined and thus not included in the promoter strength analysis.

Figure 5

Figure 5. Optimization of bisabolene production by a combinatorial approach using 7 pSensor variants and 4 production plasmid variants (pResponse). Left: Plasmid architecture of each pResponse variants. Right: Bisabolene titer after 24 and 72 hours. **(A)** Titer from pR1 production plasmid; **(B)** Titer using pR2 production plasmid; **(C)** Titer using pR3 production plasmid; **(D)** Titer using pR4 production plasmid.

Figure 6

Figure 6. Bisabolene production of genome integrated QS strains. (**A**) Two genome locations were chosen: *recA* and *poxB* to insert pS2 and pS4 QS sensor variants. RFP reporter gene driven by P_{luxI} promoter was used for characterization. The response signal from QS-integration strains are: ΔPoxB::pS2 (JBEI-7581), ΔRecA::pS2 (JBEI-7582), ΔPoxB::pS4 (JBEI-7583), ΔRecA::pS4 (JBEI-7584), and their cognate plasmid-borne QS strains: S2R0, and S4R0. (**B**) Four production plasmids (pR1 to pR4) were transformed into ΔPoxB::pS2 strain, and the bisabolene productions from these strains were measured and compared to control strain C1 and C2. C1 consists of plasmids pS0 and pC1, C2 consists of plasmids pS0 and pC2. pC1 contains P_{lacUV}-driven MevT-MBIS operon and P_{trc}-driven BIS gene, pC2 contains P_{lacUV}-driven MevT operon, P_{trc}-driven MBIS operon and P_{trc}-driven *Bis* gene. (**C**) Bisabolene production was measured in QS strains ΔPoxB::pS2 and ΔRecA::pS2. Both strains (ΔPoxB::pS2-SA and ΔRecA::pS2-SA) contains plasmids pSMevT (pJBEI-7554) and pAMBIS-Bis (pJBEI-7555).

Figure 7

36
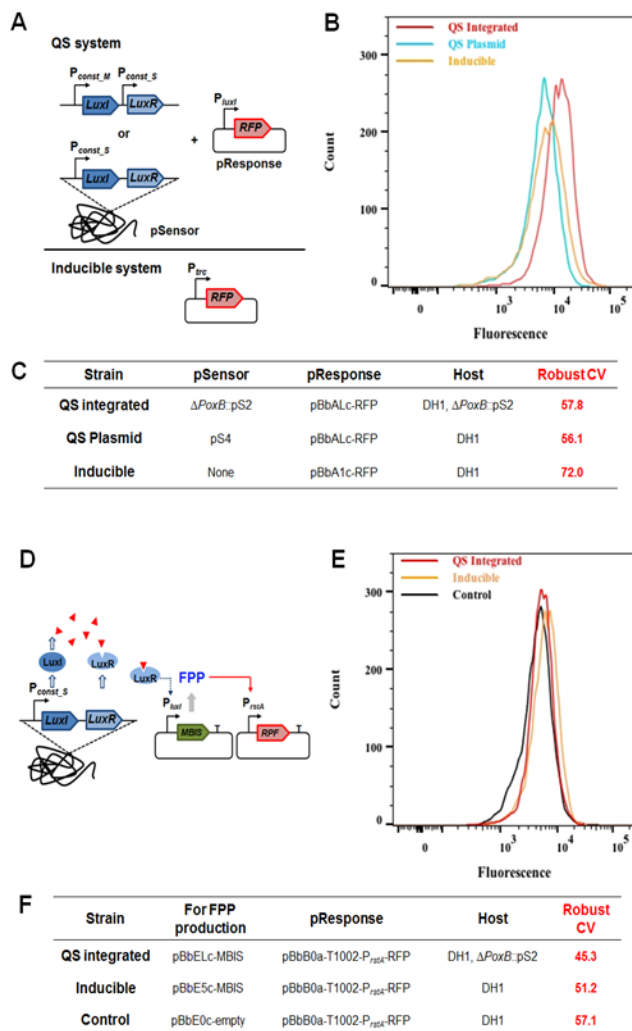
Figure 7. Analysis of the population distribution of protein expression and producing cell using flow cytometry. The fluorescence intensity of individual cells was measured by flow cytometry at 10-hr post-induction. (A) Schematics of the QS systems and IPTG-inducible system activating RFP expression. (B) RFP Fluorescence intensity and distribution spread of QS-integrated system, QS-plasmid borne system and inducible system. (C) Description of the strains and robust coefficient of variation (rCV) (D) Schematics of QS system activating the FPP biosynthesis pathway and FPP molecule activating RFP expression. (E) Fluorescence intensity and distribution spread of the QS-integrated, inducible and control systems. The QS and inducible systems contain FPP producing pathway and RFP. (F) Description of the strains and rCV.

Table 1. List of plasmids and strains

Plasmid name and Registry part number	Description	Reference (s)

pSensor

pJBEI-6481	pAC-LuxR/I	Anderson et al., 2006
pJBEI-3282 (I-pS0)	pBbA0c-empty	Lee et al., 2011
pJBEI-7492 (I-pS1)	pBbA0c-LuxR/I	This study
pJBEI-7493 (I-pS2)	pBbA0c-LuxR/I- T_{1002}-P_{trc} -Bis	This study
pJBEI-3276 (pS0)	pBbS0a-empty	Lee et al., 2011
pJBEI-7509 (pS1)	pBbS0a-P_{luxI} -LuxR-LuxI	This study
pJBEI-7510 (pS2)	pBbS0a-P_{const_S} -LuxI-LuxR	This study
pJBEI-7511 (pS3)	pBbS0a-P_{const_M} -LuxI-LuxR	This study
pJBEI-7512 (pS4)	pBbS0a-P_{const_M} -LuxI-T_{1002}- P_{const_S} -LuxR	This study
pJBEI-7513 (pS5)	pBbS0a-P_{const_W} -LuxI-LuxR	This study
pJBEI-7514 (pS6)	pBbS0a-P_{const_W} -LuxI-T_{1002}- P_{const_S} -LuxR	This study
pJBEI-7515 (pS7)	pBbS0a-P_{const_W} -LuxI-T_{1002}- P_{const_M} -LuxR	This study

pResponse

pJBEI-11741 (I-pR0)	pBbSLk-RFP	This study
pJBEI-7494 (I-pR1)	pBbSLk-MevT-MBIS-T_{1002}-P_{trc}-Bis	This study
pJBEI-7496 (pLacUV5-IpR1)	pBbSLk-MevT-T_{1006}-P_{lucUV5}-MBIS-T_{1002}-P_{trc}-Bis	This study
pJBEI-7497 (pLuxI-IpR1)	pBbSLk-MevT-T_{1006}-P_{luxI}-MBIS-T_{1002}-P_{trc}-Bis	This study
pJBEI-7527 (pC1)	pBbA5c-MevT-MBIS-T_{1002}-P_{trc}-Bis	This study
pJBEI-7528 (pC2)	pBbA5c-MevT-T_{1006}- P_{trc} -MBIS-T_{1002}- P_{trc} -Bis	This study
pJBEI-7533 (pR0)	pBbA0c- P_{luxI} -RFP	This study
pJBEI-7520 (pR1)	pBbALc-MevT-MBIS-T_{1002}- P_{trc} -Bis	This study
pJBEI-7521 (pR2)	pBbALc-MevT-T_{1006}-pLuxI-MBIS-T_{1002}- P_{trc} -Bis	This study
pJBEI-7522 (pR3)	pBbELc-MevT-MBIS-T_{1002}- P_{trc} -Bis	This study
pJBEI-7523 (pR4)	pBbELc-MevT-T_{1006}- P_{luxI} -MBIS-T_{1002}- P_{trc} -Bis	This study
pJBEI-7534 (pConst_S-RFP)	pBbA0c- P_{const_S} -RFP	This study
pJBEI-7535 (pConst_M-RFP)	pBbA0c- P_{const_M} -RFP	This study
pJBEI-7536 (pConst_W-RFP)	pBbA0c- P_{const_W} -RFP	This study
pJBEI-2488 (pLacUV5-RFP)	pBbA5c-RFP	Lee et al., 2011
pJBEI-2491 (pTrc-RFP)	pBbA1c-RFP	Lee et al., 2011

Other

pJBEI-7549	pBbB0a-T_{1002}-P_{rstA}-RFP	This study
pJBEI-7550	pBbE0c- P_{luxI} -MBIS	This study
pJBEI-7551	pBbE5c-MBIS	This study

pJBEI-7554 (pSMevT)	pBbS0c- P_{luxI} -MevT	This study
pJBEI-7555 (pAMBIS-Bis)	pBbA0a- P_{luxI} -MBIS-T1002-P_{trc}-Bis	This study
pJBEI-2997	pBbA5c-MevT-MBIS	Peralta-Yahya, 2011
pJBEI-3361	pTrc99A-Bis	Peralta-Yahya, 2011
pJBEI-3100	pBbA5c-MevT	Peralta-Yahya, 2011
pJBEI-4174	pBbS5k-MBIS-T1002-Ptrc-Bis	This study
pJBEI-3290	pBbA0c-RFP	Lee et al., 2011
pJBEI-4425	pBbE0c-RFP	Lee et al., 2011
Strain	**Descriptions**	**Reference (s)**
DH1	Base strain	Hanahan, 1983
C1	pS0 + pC1	This study
C2	pS0 + pC2	This study
I-S0R0	I-pS0 + I-pR0	This study
I-S1R0	I-pS1 + I-pR0	This study
I-QS1	I-pS1 + I-pR1	This study
I-QS2	I-pS2 + I-pR1	This study
I-QS1P$_{lacUV5}$	I-pS1 + pLacUV5-pR1	This study
I-QS1P$_{luxI}$	I-pS1 + pLuxI-pR1	This study
S0R0	pS0 + pR0	This study
S1R0	pS1 + pR0	This study
S2R0	pS2 + pR0	This study
S3R0	pS3 + pR0	This study
S4R0	pS4 + pR0	This study
S5R0	pS5 + pR0	This study
S6R0	pS6 + pR0	This study
S7R0	pS7 + pR0	This study
S1R1	pS1 + pR1	This study
S1R2	pS1 + pR2	This study
S1R3	pS1 + pR3	This study
S1R4	pS1 + pR4	This study
S2R1	pS2 + pR1	This study
S2R2	pS2 + pR2	This study
S2R3	pS2 + pR3	This study
S2R4	pS2 + pR4	This study
S3R1	pS3 + pR1	This study
S3R2	pS3 + pR2	This study
S3R3	pS3 + pR3	This study

S3R4	pS3 + pR4	This study
S4R1	pS4 + pR1	This study
S4R2	pS4 + pR2	This study
S4R3	pS4 + pR3	This study
S4R4	pS4 + pR4	This study
S5R1	pS5 + pR1	This study
S5R2	pS5 + pR2	This study
S5R3	pS5 + pR3	This study
S5R4	pS5 + pR4	This study
S6R1	pS6 + pR1	This study
S6R2	pS6 + pR2	This study
S6R3	pS6 + pR3	This study
S6R4	pS6 + pR4	This study
S7R1	pS7 + pR1	This study
S7R2	pS7 + pR2	This study
S7R3	pS7 + pR3	This study
S7R4	pS7 + pR4	This study
JBEI-7581	DH1 $\Delta poxB$::pS2	This study
JBEI-7582	DH1 $\Delta recA$::pS2	This study
JBEI-7583	DH1 $\Delta poxB$::pS4	This study
JBEI-7584	DH1 $\Delta recA$::pS4	This study
ΔPoxB::pS2-pR1	Strain pJBEI-7581 bearing pR1	This study
ΔPoxB::pS2-pR2	Strain pJBEI-7581 bearing pR2	This study
ΔPoxB::pS2-pR3	Strain pJBEI-7581 bearing pR3	This study
ΔPoxB::pS2-pR4	Strain pJBEI-7581 bearing pR4	This study
	Strain pJBEI-7581 bearing	This study
ΔPoxB::pS2-SA	pJBEI-7554 + pJBEI-7555	This study
	Strain pJBEI-7582 bearing	This study
ΔRecA::pS2-SA	pJBEI-7554 + pJBEI-7555	This study

Note: for plasmid with pBb prefix, the letters (capital and small letters) and numbers after prefix are denoted as follows. pBb: prefix; E: ColE1, A: p15A, S: SC101, B: BBR1; 0: no promoter, 1: P_{trc}, 5: P_{lacUV5}, L: P_{luxI}; a: Ampicillin resistance, c: Chloramphenicol resistance, k: Kanamycin resistance.

Highlights

- A quorum-sensing host was developed for inducer-free biofuel production in *E. coli*.
- Systematic engineering of the quorum-sensing system generated efficient QS hosts.
- Chromosomal integration of QS system generated a versatile inducer-free platform.
- The QS integrated strain produced a biofuel at higher yields than inducible system.

- QS system confirms higher homogeneity in gene expression and isoprenoid production.